

Coupled Ion-Nanomechanical Systems

L. Tian^{1,2} and P. Zoller^{1,2}

¹Institute for Theoretical Physics, University of Innsbruck, 6020 Innsbruck, Austria

²Institute for Quantum Optics and Quantum Information of the Austrian Academy of Sciences, 6020 Innsbruck, Austria

(Received 2 July 2004; published 21 December 2004)

We study ions in a nanotrap, where the electrodes are nanomechanical resonators. The ions play the role of a quantum optical system that acts as a probe and control, and allows entanglement with or between nanomechanical resonators.

DOI: 10.1103/PhysRevLett.93.266403

PACS numbers: 85.85.+j, 03.65.-w, 32.80.Pj, 85.35.Kt

Laser manipulated trapped ions are one of the prime examples of a quantum system, where control of coherent quantum dynamics, state preparation, and measurement are achieved in the laboratory, while decoherence due to coupling with the environment is strongly suppressed [1,2]. These achievements are illustrated by recent progresses in developing ion traps for quantum computing and high precision measurements [3]. A key step in the near future, which is under intensive study at the moment, is the realization and integration of ion traps with micro-fabricated nanostructures, such as segmented traps, on-chip ion traps, and mesoscopic electronic devices [4,5]. These nanostructures with their submicron size and well controlled surface properties provide strong confinement of the trapped ion and flexibility in trap design. Furthermore, the integration of ion traps with nanostructures opens a novel way of studying the quantum properties of the nanomechanical motions of the nanostructures; i.e., the ions act as a powerful tool in probing and manipulating the quantum modes of the mesoscopic systems. In addition, this raises interesting questions concerning decoherence of ion trap qubit in a solid state environment due to electrical and mechanical noise on the electrodes, and provides a new tool to study these interactions. The manipulation of quantum states of motional degrees of freedom of nanomechanical systems has been discussed previously in the context of laser manipulated quantum dots embedded in cantilevers [6], vibrations of mirrors via their interaction with photons in a high finesse cavity [7], and via coupling with electronic devices such as single electron transistor [8] and superconducting charge qubits [9].

In this Letter we study ions in a mesoscopic Paul trap, where suspended nanomechanical resonators [10] play the role of tiny trap electrodes and act as high- Q nanomechanical resonators with their own quantum degrees of freedom. Below we develop a model of the trapped ions coupled with the flexural modes of these nanomechanical electrodes. In particular, we investigate the possibility of manipulation, preparation, and measurement of quantum states of the flexural modes via the laser driven ion in the limit where the trapping frequency of the ion is resonant with the frequency of the nanomechanical oscillator. This setup can be generalized to ion trap and nanoelectrode

arrays. Another application is quantum computing, where mesoscopic traps not only promise very strong confinement and an associated speed up of two-qubit quantum gates, but also coupling via the nanomechanical electrodes offers new ways of entangling internal states of ions. We also study the decoherence mechanism for the trapped ions due to the nanomechanical and electrical couplings which introduce quantum Brownian motion of the electrodes and limit the ability of manipulating the mechanical modes via the ion.

Model of ion coupled to nanomechanical electrodes.—A schematic setup is illustrated in Fig. 1, where an ion is trapped between two parallel suspended electrodes represented by nanowires or nanotubes [10]. When a gate voltage $V(t) = V_0 \cos \omega_{ac} t$ with frequency ω_{ac} is applied to the electrodes via Ohmic contacts, the charge on the electrodes oscillates with time and leads to oscillating forces on the ion as well as between the electrodes. Averaging over the fast driving frequency results in an effective harmonic trapping potential for the ion centered between the electrodes. In Fig. 1, the electrodes are separated by a distance of $2d_0 = 200 \mu\text{m}$ with $2d_0$ much shorter than their length $2L_0$ and are located a distance $h_0 (\leq L_0)$ above the ground plane. As a consequence, there will be tight trapping of the motion of the ion along the x axis which is the motion coupling to the high- Q flexural (bending) vibrations of the electrodes. The confinement in the orthogonal directions is much looser.

The flexural vibration $u_i(y)$ of the i th electrodes can be expanded as $u_i(y) = \sum_n \hat{X}_{in} u_{in}(y)$ where \hat{X}_{in} is the quan-

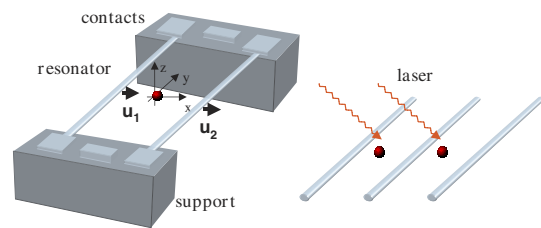


FIG. 1 (color online). Setup. Left: ion trap with electrodes made of nanomechanical resonators suspended above ground and biased with ac voltage; right: arrays of nanomechanical resonators and laser manipulation of the trapped ions.

tized coordinate of the n th flexural modes with the conjugate momentum \hat{P}_{in} and $u_{in}(y)$ is the eigenfunction of the n th flexural mode with wave vector q_{in} and frequency $\omega_{in} = \sqrt{EI_2/\rho q_{in}^2}$. Here E is Young's modulus, I_2 the moment of inertia, and ρ the mass density of the electrodes [8,10,11]. Other acoustic phonons at long wavelength are the longitudinal modes and the torsional modes which have much higher frequencies than that of the flexural modes. The lowest flexural mode, also called the fundamental mode, has $q_{i1} \approx (2\pi/L_0)0.376$. For nanowires with a length of the order of μm the fundamental frequencies are in the range of tens to a few hundred MHz; for a carbon nanotube [10,12] with the Young's modulus $E = 1 \text{ TPa}$ and length $2L_0 = 500 \text{ nm}$, the fundamental frequency is $\omega_b \approx 1 \text{ GHz}$.

We study the coupling between the ion motion along the x axis and that of the fundamental modes of the electrodes, which is caused by the Coulomb interaction between the ion and the charge distribution on the electrodes. As derived below, the Hamiltonian of the combined ion-nanomechanical system after adiabatically eliminating the fast (micro-)motion at the drive frequency ω_{ac} has the form of coupled harmonic oscillators,

$$H_{\text{eff}} = \hbar\omega_\nu \hat{a}^\dagger \hat{a} + \sum_i \hbar\omega_{bi} \hat{b}_i^\dagger \hat{b}_i + i\lambda \sum_i (\alpha_i \hat{b}_i^\dagger \hat{a} + \text{H.c.}), \quad (1)$$

where \hat{b}_i (\hat{b}_i^\dagger) and \hat{a} (\hat{a}^\dagger) are the lowering (raising) operators of the fundamental mode \hat{X}_{i1} with $i = 1, 2$ and the motion of the ion, respectively, with ω_{bi} the frequency of \hat{X}_{i1} and ω_ν the trapping frequency of the ion. When $\omega_\nu \sim \omega_b \ll \omega_{ac}$, the trapping frequency is $\omega_\nu = q_0 V_0 / \sqrt{2d_0^2 m \omega_{ac}}$, depending on the renormalized driving voltage $\tilde{V}_0(t) = 2V(t) / \ln(2h_0 \sqrt{h_0^2 + d_0^2} / r_0 d_0)$ with r_0 the radii of the electrodes. The coupling is $\lambda = \hbar\omega_\nu u_0 \sqrt{m/M_p}$, where m and M_p are mass of the ion and the total mass of the two electrodes, respectively, and $u_0 = u_{i1}(y=0)$. For symmetric electrodes $\alpha_{1,2} = 1/2$. The coupling is proportional to the trapping frequency while reduced by the mass ratio m/M_p , which shows that nanomechanical resonators with light mass, e.g., a single wall carbon nanotube, have stronger coupling. With the parameters $V_0 = 5 \text{ V}$, $\omega_{ac}/2\pi = 3 \text{ GHz}$, $d_0 = 100 \text{ nm}$, $h_0 = 10d_0$, $r_0 = 2 \text{ nm}$, $m/M_p = 10^{-4}$, we have $\omega_\nu/2\pi = 1 \text{ GHz}$ and $\lambda = 10 \text{ MHz}$.

The Hamiltonian (1) is derived by expanding the Coulomb interaction between the ion and the charge on the electrodes, and Coulomb repulsion between the electrodes, taking into account the displacement of the ion \hat{x} and the motion of the electrodes \hat{X}_{i1} ($i = 1, 2$). The charge distribution on the i th electrodes includes an (essentially uniform) charge density $\rho_{iv}(t) = \rho_{iv} \cos \omega_{ac} t$ induced by the external voltage, and an "image charge" density ρ_{iq} due to the presence of the ion [13]. When $h_0 \gg d_0$, the small correction to the trapping potential and the coupling caused by the "image" charge can be neglected. Up to

second-order expansion in the displacements, the Coulomb energy of the electrodes includes a static force on the electrodes with the form $\sum g_{in}^{(1)} \cos(\omega_{ac} t) \hat{X}_{in}$, the interaction between modes of the same electrodes $\sum h_{i,mn}^{(2)} \cos(\omega_{ac} t) \hat{X}_{im} \hat{X}_{in}$, and the interaction between modes on different electrodes $\sum \kappa_{ij,mn}^{(2)} \cos^2(\omega_{ac} t) \hat{X}_{im} \hat{X}_{jn}$. The Coulomb energy of the ion includes the trapping potential $q_0 \tilde{V}_0(t) \hat{x}^2 / 2d_0^2$, and the coupling between the ion and the fundamental modes $\sum g_{in}(t) \hat{X}_{in} \hat{x}$. Explicit expression for the coefficients of the electrodes can be derived from an expansion of the electrostatic energy $E_m = -\frac{1}{2} \sum_{i,j} C_{ij} \{\hat{X}_{in}\} V_i V_j$ for given applied voltages $V_i [= V(t)]$, with C_{ij} capacitances of the resonators as functions of the displacements. For an array of electrodes, as in Fig. 1, these coupling terms may (partially) compensate each other due to symmetry considerations. It can be shown that with the parameter given in this Letter, the terms $g_{in}^{(1)}$, $h_{i,mn}^{(2)}$, and $\kappa_{ij,mn}^{(2)}$ are much smaller than the elastic energy $\hbar\omega_{bi}$ and are neglected from Eq. (1). The coupling g_{in} has the form $g_{in}(t) = g_{in} \cos \omega_{ac} t$ with

$$g_{in} = \int_i dy \frac{q_0 \rho_{iv}(t) (y^2 - 2d_0^2) u_{in}(y)}{4\pi\epsilon_0 (d_0^2 + y^2)^{5/2}}$$

being a rapidly decreasing function of n .

Hence, when the trap frequency is near resonant with the fundamental modes and the driving frequency ω_{ac} is far off resonant with any elastic eigenmodes, the single mode approximation for the vibration of the electrodes applies with the Coulomb energy of the ion as $q_0 \tilde{V}_0(t) \times [\hat{x} - u_{11}(0) \hat{X}_p]^2 / 2d_0^2$ where $\hat{X}_p = \alpha_1 \hat{X}_{11} + \alpha_2 \hat{X}_{21}$. This energy has the simple interpretation of a parametric oscillator with the trap center located at the center-of-mass (c.m.) displacement \hat{X}_p , providing a bilinear coupling of the ion to the electrodes. Eliminating the micro-motion, we obtain the Hamiltonian (1).

The coupled oscillator Hamiltonian (1) allows the exchange of phonons of the ion and nanomechanical motion. Motional states of the ions can be manipulated by coupling internal electronic states to a laser: $H_I = -\frac{1}{2} \delta \sigma_z + \Omega e^{i\eta(a+a^\dagger)} \sigma^+ + \text{H.c.}$, which can be added to Eq. (1). Here σ 's are the Pauli operators of the a two-state system, δ the laser detuning, Ω the Rabi frequency, and $\eta = k\sqrt{\hbar/2m\omega_\nu}$ the Lamb-Dick parameter describing the laser recoil on the ion motion. A complete toolbox hence is available on the ion [14] for (i) quantum state engineering of the motional state, (ii) preparation of pure states (ground state cooling), and (iii) state detection using the quantum jump technique. Preparing and analyzing motional states of the resonators are available via the transfer Hamiltonian when the coupling time $1/\lambda$ is faster than the decoherence time. Below we show two examples of exploring the quantum features of the nanomechanical modes of the electrodes via laser manipulation of the ion.

Entanglement generation.—As an illustration of the manipulation of nanomechanical modes, we give a protocol for the entanglement generation [1,2,9] between the fundamental modes of the electrodes (as a continuous variable system) via laser control of the ion and the bilinear coupling in Eq. (1). Consider two electrodes that have different fundamental frequencies with $|\omega_{b1} - \omega_{b2}| \gg \lambda$. The couplings between the ion and the fundamental modes are $\lambda_i = \alpha_i \lambda$ respectively with $i = 1, 2$. Below we present a scheme that generates the state $|\psi_1, \chi_2\rangle + |\chi_1, \psi_2\rangle$ for the two fundamental modes, where $|\psi_i\rangle$ and $|\chi_i\rangle$ are arbitrary states of the electrode. For coherent states with $\langle\chi_i|\psi_j\rangle \sim 0$, maximal entanglement is generated between the fundamental modes.

We start with the initial state $(|\uparrow, \psi_x\rangle + |\downarrow, \chi_x\rangle)|0_1, 0_2\rangle$ where the index x refers to the motional mode of the ion and 1, 2 refer to the modes of the electrodes. This state can be prepared using standard protocols of the ion trap qubits [15] so that the motional and the internal mode of the ion are entangled while the modes of the electrodes are in their ground state. In a first step we tune the trapping frequency of the ion to be resonant with that of the first electrode: $\omega_\nu = \omega_{b1}$ for a duration of $\pi/2\lambda_1$. This results in the swap of the states of the motion of the ion and the first electrode: $|n_x, m_1\rangle \rightarrow |m_x, n_1\rangle$, and the state is now $(|\uparrow, 0_x, \psi_1\rangle + |\downarrow, 0_x, \chi_1\rangle)|0_2\rangle$. Now prepare the ion state once more to obtain the state $(|\uparrow, \chi_x, \psi_1\rangle + |\downarrow, \psi_x, \chi_1\rangle)|0_2\rangle$. This can be achieved by flipping each of the internal modes to a third internal mode to hide this mode from the laser pulses while preparing the motional state of the other internal mode [15]. Then, tune the trapping frequency to $\omega_\nu = \omega_{b2}$ for a duration of $\pi/2\lambda_2$, which results in the swap of the states of the motion of the ion and the second electrode: $|n_x, m_2\rangle \rightarrow |m_x, n_2\rangle$, and the state is now $(|\uparrow, 0_x, \psi_1, \chi_2\rangle + |\downarrow, 0_x, \chi_1, \psi_2\rangle)$. Now, rotate the internal mode by a $\pi/2$ pulse that achieves the transformation: $|\uparrow\rangle \rightarrow |\uparrow\rangle + |\downarrow\rangle$ and $|\downarrow\rangle \rightarrow |\uparrow\rangle - |\downarrow\rangle$. Finally, detect the internal state which generates the states $|\psi_1, \chi_2\rangle \pm |\chi_1, \psi_2\rangle$ depending on the detected internal mode. Hence entanglement is transferred from the internal mode and the motional mode of the ion to the modes of the electrodes.

This method can be applied to generate, for example, $|0_1, 1_2\rangle + |1_1, 0_2\rangle$, an entangled state of the two electrode modes. The entanglement can be achieved on a time scale of $\pi/\lambda_{1,2} \approx 50$ ns, which is much shorter than the decoherence time due to the quality factor, given the quality factors approaching $Q \geq 10^5$ of the nanomechanical modes measured in experiments [8]. With $Q \geq 10^3$ and neglecting the voltage noise (see below), a fidelity of $\exp(-1/20)$ can be achieved for the entanglement.

Cooling of the nanomechanical modes via the ion.—A crucial step in quantum state engineering is the preparation of pure states, and hence laser cooling. Tuning a laser below the optical resonance frequency of the ion will excite the ion while absorbing a phonon from the ion motion. In the subsequent spontaneous emission the ion returns to the electronic ground state. Repeating this opti-

cal pumping leads to ground state cooling of the ion, provided that the spontaneous emission rate of the ion is much less than the trap frequency (the sideband cooling limit [14]). In the case of an ion coupled to a nanomechanical electrode, phonons of the electrodes can be swapped to the ion according to the Hamiltonian (1), and thus will be cooled by the ion. For simplicity, we study the situation of symmetric electrodes, $\omega_{bi} = \omega_b$, and the cooling of the c.m. motion of the electrodes.

The cooling mechanism is illustrated in Fig. 2 where the energy structure of the coupled ion and electrode system is plotted. The states are labeled as $|s, n, m\rangle$, corresponding to the internal state s , the number state n of the motion of the ion, and the number state m of the electrode mode. Three paths lead to the cooling of the electrodes. For example, one cooling path in Fig. 2 starts with the laser pumping between the states $|s, n, m\rangle$ and $|\bar{s}, n-1, m\rangle$, then the spontaneous emission from the state $|\bar{s}, n-1, m\rangle$ to the state $|s, n-1, m\rangle$, and finally the transfer between the states $|s, n-1, m\rangle$ and $|s, n, m-1\rangle$, which reduced the phonon number of the electrode. The three heating paths in the laser cooling process are off resonance processes with a much weaker effect than that of the cooling paths. In addition, other heating effects can be induced by the mechanical and electrical noise on either the ion or the electrodes. The mechanical noise on the electrodes is characterized by the finite quality factor and induces a relaxation and heating of the electrodes towards the thermal temperature with the rate $\Gamma_\nu = \omega_b/Q$. The electrical noise is described as voltage fluctuations with the decoherence rate γ_m , where the dominate decoherence effect is induced by a linear coupling of the fluctuations to the ion motion \hat{x} . The decoherence rate γ_m of the linear coupling depends on circuit resistances and the geometry of the electrodes, and can be avoided as discussed below.

By solving the master equation of the laser cooling and eliminating the internal modes of the ion [16], the final phonon number of the electrode is:

$$\langle \hat{b}^\dagger \hat{b} \rangle = \frac{[\Gamma_\nu \gamma_{\text{eff}}^{\hat{a}} (\gamma_{\text{eff}}^{\hat{a}} + \Gamma_\nu) + 4\Gamma_\nu \lambda^2] n_B + 4\gamma_{\text{eff}}^{\hat{a}} \lambda^2 n_f^{\text{eff}}}{(\Gamma_\nu + \gamma_{\text{eff}}^{\hat{a}})(\gamma_{\text{eff}}^{\hat{a}} \Gamma_\nu + 4\lambda^2)}$$

with the assumption that the ion reaches its ground state by the laser cooling in the absence of the electrodes. The

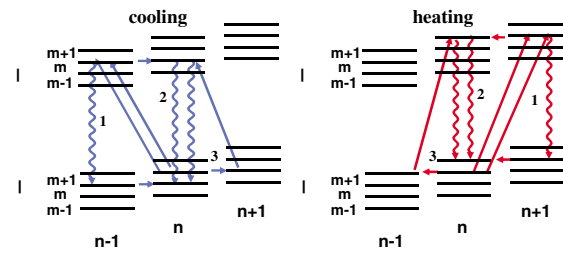


FIG. 2 (color online). Energy structure of the coupled system of the ion and the electrodes. Left: cooling circles; right: heating circles.

effective cooling rate of the electrodes is $\gamma_{\text{eff}}^{\hat{a}} = \gamma_{\omega}^{\hat{a}} + \gamma_m$ with $\gamma_{\omega}^{\hat{a}}$ the rate of laser cooling of the ion, and the final phonon number of the ion is $n_f^{\text{eff}} = n_B \gamma_m / \gamma_{\text{eff}}^{\hat{a}}$. It is obvious when $\gamma_m \sim \gamma_{\omega}^{\hat{a}}$ that the ion is not cooled and neither is the electrode mode. When $\gamma_m \sim 0$, avoiding the linear coupling, the minimal stationary phonon number is

$$\langle \hat{b}^\dagger \hat{b} \rangle = \frac{k_B T (4\lambda + \Gamma_\nu)}{Q(2\lambda + \Gamma_\nu)^2} \quad (2)$$

at $\gamma_{\omega}^{\hat{a}} = 2\lambda$. At a temperature of $T = 4$ K, the thermal phonon number is 100 for $\omega_b = 1$ GHz. With our parameters: $\Gamma_e = 5$ MHz, $\Omega_r = 300$ MHz, and $\gamma_{\omega}^{\hat{a}} = 2$ MHz $< 2\lambda$, we have $\langle \hat{b}^\dagger \hat{b} \rangle_f \approx 0.5$ assuming $Q = 10^5$.

For the high trapping frequencies discussed above, the Lamb-Dicke parameter is small with $\eta \sim 0.01$. As a result, $\gamma_{\omega}^{\hat{a}} < \lambda$ and the cooling rate of the ion becomes the bottleneck that limits the cooling of the electrodes. The problem can be avoided by trapping the ion at low frequency $\omega_\nu \ll \omega_b \sim \omega_{\text{ac}}$ (and thus large η). The ac driving field provides a parametric up-conversion of the ion to the resonator phonons, i.e., $\lambda \rightarrow \hbar \omega_\nu u_1 \sqrt{m \omega_{\text{ac}}^2 / M_p \omega_b \omega_\nu} e^{-i\omega_{\text{ac}} t}$ in Eq. (1).

Decoherence.—The coupled ion and electrode system is subject to both the mechanical noise [11] described by the quality factor Q and the electrical noise represented as voltage fluctuations in the circuit. The quality factor has reached 10^3 in recent experiments [8], which at low temperature of 40 mK gives $k_B T / Q <$ MHz. The electrical noise includes the noise of the resistances in the circuit, shot noise, and low frequency noise ($1/f$ noise) [17]. In our setup for a ballistic electrode such as single wall carbon nanotube at $\omega_\nu = 1$ GHz, the dominate noise is induced by the contact resistances in the circuit.

Let $\delta \tilde{v}_{1,2}(t)$ be the normalized voltage noise on the electrodes defined the same way as \tilde{V}_0 . This generates both parametric noise that couples with the ion as $q_0 [\delta \tilde{v}_1(t) + \delta \tilde{v}_2(t)] \hat{x}^2 / 4d_0^2$ and the linear noise as $q_0 [\delta \tilde{v}_1(t) - \delta \tilde{v}_2(t)] \hat{x} / 4d_0$. For Ohmic contact, the contact resistance is $R_c = h / 2N_\perp e^2$ with N_\perp the number of conducting channels. For single wall carbon nanotube, $N_\perp = 4$ and $R_c = 3000 \Omega$. In this case, the parametric noise generates a decoherence rate of 0.5 Hz for uncorrelated noise, which is a small effect as its spectrum is proportional to $(\delta x_0 / d_0)^4$ and $\delta x_0 / d_0 \ll 1$, where $\delta x_0 = \sqrt{\hbar / 2m \omega_\nu}$. The linear noise, on the other hand, has a much stronger effect as it is only proportional to $(\delta x_0 / d_0)^2$. Assuming the noise is uncorrelated, $(\delta \tilde{v}_1 - \delta \tilde{v}_2)^2(\omega) = \delta \tilde{v}_1^2(\omega) + \delta \tilde{v}_2^2(\omega)$, which gives a decoherence rate of 0.5 MHz. However, when $\delta \tilde{v}_1 = \delta \tilde{v}_2$, $(\delta \tilde{v}_1 - \delta \tilde{v}_2)^2(\omega) = 0$ where the linear noise disappears. To make sure that the voltage fluctuations are correlated: $\tilde{v}_1 = \tilde{v}_2$, we choose a geometry where the electrodes are built from one piece of metal bent into two branches, e.g., a bent nanotube where there is only one contact in the middle of the metallic electrode.

Quantum Computing.—We have demonstrated with two examples that the laser controlled trapped ions can be a

powerful tool in studying the nanomechanical modes of nanowires or nanotubes. At the same time, coupling the ion with nanowires or nanotubes promises high speed ion trap with frequencies significantly higher than those of present ion traps and hence an associated speed up of two-qubit gates in ion trap quantum computing (Fig. 1) [1]. The standard two-qubit protocols based on, for example, entanglement via a phonon data bus or a push gate [4] are readily adapted to the present case. In the second case, gate times of the order of nanoseconds seem possible for the numbers above. An alternative is entanglement via exchange of phonons of one of the collective ion-electrode modes of the system. Note additional noise is introduced by the nanomechanical motion and its coupling with the ion. The decoherence time can be significantly increased, however, by tuning the trapping frequency off resonance with that of the electrode modes.

We thank M. S. Dresselhaus, B. I. Halperin, D. Leibfried, L. S. Levitov, M. D. Lukin, A. S. Sørensen, and W. Zwerger for helpful discussions. This work is supported by the Austrian Science Foundation, European Networks and the Institute for Quantum Information.

- [1] J. I. Cirac and P. Zoller, Phys. Today **57**, No. 3, 38 (2004).
- [2] D. J. Wineland *et al.*, J. Res. Natl. Inst. Stand. Technol. **103**, 259 (1998).
- [3] M. D. Barrett *et al.*, Nature (London) **429**, 737 (2004); M. Riebe *et al.*, Nature (London) **429**, 734 (2004).
- [4] D. Kielpinski *et al.*, Nature (London) **417**, 709 (2002); J. I. Cirac and P. Zoller, Nature (London) **404**, 579 (2000).
- [5] L. Tian *et al.*, Phys. Rev. Lett. **92**, 247902 (2004); A. S. Sørensen *et al.*, Phys. Rev. Lett. **92**, 063601 (2004).
- [6] I. Wilson-Rae, P. Zoller, and A. Imamoğlu, Phys. Rev. Lett. **92**, 075507 (2004).
- [7] W. Marshall *et al.*, Phys. Rev. Lett. **91**, 130401 (2003); S. Mancini *et al.*, Phys. Rev. Lett. **88**, 120401 (2002).
- [8] M. D. LaHaye *et al.*, Science **304**, 74 (2004); R. G. Knobel and A. N. Cleland, Nature (London) **424**, 291 (2003).
- [9] A. D. Armour, M. P. Blencowe, and K. C. Schwab, Phys. Rev. Lett. **88**, 148301 (2002); E. K. Irish and K. Schwab, Phys. Rev. B **68**, 155311 (2003).
- [10] A. Husain *et al.*, Appl. Phys. Lett. **83**, 1240 (2003); P. Poncharal *et al.*, Science **283**, 1513 (1999); B. Babic *et al.*, Nano Lett. **3**, 1577 (2003).
- [11] A. N. Cleland and M. L. Roukes, J. Appl. Phys. **92**, 2758 (2002).
- [12] R. Saito *et al.*, *Physical Properties of Carbon Nanotubes* (Imperial College Press, London, 1998); Special issue on Advances in Carbon Nanotubes, edited by M. S. Dresselhaus and H. Dai, [MRS Bull. **29**, No. 4, (2004)].
- [13] B. E. Granger *et al.*, Phys. Rev. Lett. **89**, 135506 (2002).
- [14] D. Leibfried *et al.*, Rev. Mod. Phys. **75**, 281 (2003).
- [15] C. K. Law and J. H. Eberly, Phys. Rev. Lett. **76**, 1055 (1996); J. I. Cirac and P. Zoller, Phys. Rev. Lett. **74**, 4091 (1995).
- [16] J. I. Cirac *et al.*, Phys. Rev. A **46**, 2668 (1992).
- [17] Ya. M. Blanter and M. Büttiker, Phys. Rep. **336**, 1 (2000).